JBC ARTICLE

Histone deacetylase 3 preferentially binds and collaborates with the transcription factor RUNX1 to repress AML1–ETO–dependent transcription in t(8;21) AML

Received for publication, August 18, 2019, and in revised form, February 11, 2020 Published, Papers in Press, February 18, 2020, DOI 10.1074/jbc.RA119.010707

Chun Guo[‡], Jian Li[‡], Nickolas Steinauer[‡], Madeline Wong[‡], Brent Wu[‡], Alexandria Dickson[‡], Markus Kalkum[§], and Jinsong Zhang[‡1]

From the [‡]Department of Pharmacology and Physiology, Saint Louis University, School of Medicine, St. Louis, Missouri 63104 and the [§]Department of Molecular Imaging and Therapy, Beckman Research Institute of the City of Hope, Duarte, California 91010

Edited by Joel M. Gottesfeld

In up to 15% of acute myeloid leukemias (AMLs), a recurring chromosomal translocation, termed t(8;21), generates the AML1–eight–twenty-one (ETO) leukemia fusion protein, which contains the DNA-binding domain of Runt-related transcription factor 1 (RUNX1) and almost all of ETO. RUNX1 and the AML1–ETO fusion protein are coexpressed in t(8;21) AML cells and antagonize each other's gene-regulatory functions. AML1–ETO represses transcription of RUNX1 target genes by competitively displacing RUNX1 and recruiting corepressors such as histone deacetylase 3 (HDAC3). Recent studies have shown that AML1–ETO and RUNX1 co-occupy the binding sites of AML1–ETO–activated genes. How this joined binding allows RUNX1 to antagonize AML1–ETO–mediated transcriptional activation is unclear. Here we show that RUNX1 functions as a *bona fide* repressor of transcription activated by AML1–ETO. Mechanistically, we show that RUNX1 is a component of the HDAC3 corepressor complex and that HDAC3 preferentially binds to RUNX1 rather than to AML1–ETO in t(8;21) AML cells. Studying the regulation of interleukin-8 (*IL8*), a newly identified AML1–ETO–activated gene, we demonstrate that RUNX1 and HDAC3 collaboratively repress AML1–ETO–dependent transcription, a finding further supported by results of genome-wide analyses of AML1–ETO–activated genes. These and other results from the genome-wide studies also have important implications for the mechanistic understanding of gene-specific coactivator and corepressor functions across the AML1–ETO/RUNX1 cistrome.

This work was supported by National Institutes of Health Grants R01HL093195 (to J. Z.), R21CA178513 (to J. Z.), President's Research fund from Saint Louis University (to J. Z.), Siteman Investment Program (SIP) Award from the Siteman Cancer Center at Barnes-Jewish and Washington University School of Medicine (to J. Z.) and National Institutes of Health Grant T32GM008306-26A1 (to N. S.) The Mass Spectrometry and Proteomics Core facility of City of Hope was supported in part by the NCI, National Institutes of Health under Award P30CA033572 (to M. K.). The authors declare that they have no conflicts of interest with the contents of this article. The content is solely the responsibility of the authors and does not necessarily represent the official views of the National Institutes of Health.

This article contains Figs. S1–S7, Supporting Information S1–S2 and Table S1.

The ChIP-Seq results have been deposited into the GEO under accession number GSE131939. The mass spectrometry proteomics data have been deposited into the ProteomeXchange Consortium via the PRIDE partner repository with the dataset identifiers PXD017230 and 10.6019/PXD017230.

[1] To whom correspondence should be addressed. Tel.: 314-977-6496; E-mail: jinsong.zhang@health.slu.edu.

The t(8;21) chromosomal translocation generates the AML1–ETO[2] fusion protein, which combines the Runt homology DNA-binding domain derived from the RUNX1/AML1 gene with a nearly full-length ETO (also known as MTG8, RUNX1T1, or CBFA2T1) (1). AML1–ETO and the ETO family of proteins contain four distinct Nervy homology regions (NHR1–NHR4), which share homology with the corresponding regions in the *Drosophila* Nervy protein. These NHRs play roles in protein–protein interactions (2). NHR1 and NHR2 are involved in binding to E-proteins (3–5), which belong to the basic helix–loop– helix family of sequence-specific transcription factors. NHR1 is also engaged in interactions with the p300 histone acetyltransferase (6) whereas NHR2 is engaged in oligomerization (2). NHR4 contains two myeloid translocation protein 8, Nervy, and DEAF-1 (MYND)–type zinc fingers that bind to nuclear receptor corepressors (NCoR/NCoR1 and SMRT/NCoR2, collectively called CoRs) and, in turn, to HDACs (7–9). NCoR and SMRT interact with HDAC3 to form stoichiometric complexes that also contain Transducin β-like 1 (TBL1)/TBL1-like protein 1 (TBLR1) and G protein pathway suppressor 2 (GPS2) subunits (10). In these complexes, CoRs directly bind and activate the latent enzymatic activity of HDAC3 (10, 11). These studies indicate that AML1–ETO indirectly binds to HDAC3 through the CoR subunit of the HDAC3 complex.

AML1–ETO can repress and activate transcription of different target genes. At least two mechanisms have been proposed for AML1–ETO–mediated repression. First, AML1–ETO competes with RUNX1 for DNA binding, displacing RUNX1 and exchanging RUNX1-associated coactivators with AML1–ETO–associated CoR/HDAC corepressors (7–9). Second, AML1–ETO directly binds to the activation domains of E-proteins (4). Through this activity, it precludes binding of coactivators, including GCN5, to E-proteins (3, 12, 13). AML1–ETO–mediated activation, on the other hand, is associated with recruitment of coactivator proteins such as p300 (6, 14–16).

[2] The abbreviations used are: ETO, eight–twenty-one; AML, acute myeloid leukemia; NHR, Nervy homology region; NCoR, nuclear receptor corepressor; SMRT, silencing mediator for retinoid and thyroid-hormone receptors; HDAC, histone deacetylase; ChIP-Seq, ChIP sequencing; RT-qPCR, quantitative RT-PCR; TSA, Trichostatin A; rep, repressed; act, activated; CoR, corepressor.

© 2020 Guo et al. Published under exclusive license by The American Society for Biochemistry and Molecular Biology, Inc.

Although it is well-known that AML1–ETO deregulates gene transcription to promote leukemogenesis, the mechanistic details of AML1–ETO–mediated transcriptional activity have not been fully elucidated. For example, it has been thought that competition of DNA binding by AML1–ETO and RUNX1 is a major mechanism underlying their functional crosstalk (17–20). However, emerging evidence suggests that, although AML1–ETO and RUNX1 may compete for DNA binding on genes that are repressed by AML1–ETO, the gene-regulatory loci that are activated by AML1–ETO are permissive for RUNX1/AML1–ETO co-occupancy (16). This finding has led to the proposal that, because RUNX1 is a transcriptional activator, the activation effect of AML1–ETO may be attributed to its ability to recruit additional activation signals beyond that provided by RUNX1 (21). However, if both AML1–ETO and RUNX1 function as activators in this context, then it is difficult to explain how RUNX1 may negate the activation effect of AML1–ETO at these genes. It should be mentioned that, although RUNX1 has been commonly viewed as a transcriptional activator in t(8;21) AML cells, there are reports that it can also bind to corepressors such as Sin3A and HDACs (22–24). However, the specificity of these interactions and their potential roles in regulating gene expression in t(8;21) AML cells have not been explored.

In this study, we found that, independent of the interaction between AML1–ETO and HDAC3, RUNX1 also has the ability to bind to HDAC3 in complex with CoRs. Moreover, comparative affinity pulldown assays showed that HDAC3 has a higher binding affinity for RUNX1 than for AML1–ETO in t(8;21) AML cells. Additional studies focusing on a newly discovered HDAC3 target gene (*IL8/CXCL8*) led to the discovery that RUNX1 also has the ability to collaborate with HDAC3 to repress AML1–ETO–mediated activation of gene transcription. These results indicate that HDAC3 facilitates bidirectional negative interplays between AML1–ETO and RUNX1. Furthermore, pairwise ChIP-Seq studies performed in t(8;21) AML cells with and without AML1–ETO depletion provided evidence of the presence of RUNX1–HDAC3 complexes at genome-wide AML1–ETO target genes and new mechanistic insights into the roles of AML1–ETO and RUNX1, along with coactivators and corepressors, in regulating gene transcription in t(8;21) AML.

Results

Identification of IL8 as an HDAC3 target gene

We examined HDAC3-regulated genes in Kasumi-1 t(8;21) AML cells by performing RNA-Seq analyses following depletion of HDAC3. Using cutoffs of $p \leq 0.05$ and fold change ≥ 2.5, we identified 77 HDAC3– down-regulated genes and 102 HDAC3– up-regulated genes (Fig. 1*A*) whose expression was up-regulated (shHDAC3-up) and down-regulated (shHDAC3-down) by knocking down HDAC3 (Fig. 1*A*). Validating the RNA-Seq results, Gene Ontology studies showed that HDAC3–down-regulated genes were enriched with genes up-regulated in AML1–ETO– depleted Kasumi-1 cells, consistent with the cooperative functions of HDAC3 and AML1–ETO in repression (7–9), as well as genes regulating immune and inflammatory functions known to be associated with HDAC3 (25, 26) (Fig. 1*A*). Interestingly, HDAC3– up-regulated genes were associated with cell movement and WNT pathways (Fig. 1*A*).

A proinflammatory gene, *IL8/CXCL8* (27), showed the most significant up-regulation upon depletion of HDAC3 in Kasumi-1 cells (Fig. 1*B*, fold change = 18.12, $p = 7.3E-08$) and was chosen for further mechanistic studies. RT-qPCR assays confirmed the ability of HDAC3 to regulate IL8 and showed that the regulation is specific for both IL8 and HDAC3 (Fig. 1, *C–E*). Depleting HDAC3, but not HDAC1, strongly up-regulated IL8 but not PADI1, whereas depleting HDAC1 showed the opposite effects (Fig. 1*C*). Furthermore, depleting HDAC3-interacting CoRs or inactivating deacetylase activities also up-regulated IL8 in Kasumi-1 cells (Fig. 1*D*). Further supporting a role for HDAC3 in inhibiting IL8 gene expression, ectopic expression of HDAC3 down-regulated IL8 expression in Kasumi-1 cells (Fig. 1*E*).

HDAC3 regulation of IL8 is t(8;21) translocation– dependent

We next asked whether the ability of HDAC3 to down-regulate IL8 can be generalized to other cell types. Although depleting HDAC3 similarly up-regulated IL8 in SKNO-1 t(8;21) cells, no such effects were observed in non-t(8;21) cells (Fig. 1*F*).

AML1–ETO activates IL8 gene transcription

Given that HDAC3 has been shown to collaborate with AML1–ETO, AML1–ETO may mediate the repressive effect of HDAC3 on IL8. Unexpectedly, depleting AML1–ETO decreased, rather than increased, IL8 expression (Fig. 2*A*, *left panels*). This was also confirmed using another AML1–ETO–specific shRNA (Fig. S1*A*). In overexpression studies, ectopic AML1–ETO increased IL8 expression in Kasumi-1 cells (Fig. 2*A*, *right panels*). This result prompted us to test whether AML1–ETO has an intrinsic ability to activate IL8 transcription. Confirming this idea, ectopic expression of AML1–ETO dramatically enhanced IL8 gene expression in U937 AML cells (Fig. 2*B*).

HDAC3 regulation of IL8 is RUNX1-dependent

As mentioned earlier, RUNX1 is thought to function as a constitutive activator on both AML1–ETO–repressed and AML1–ETO–activated genes. However, depletion of RUNX1 increased, rather than decreased, IL8 gene expression in Kasumi-1 cells (Fig. S1*B*). Consistently, overexpression of RUNX1 reduced IL8 gene expression (Fig. 2*C*). These results prompted us to further study the cross-talk between RUNX1, AML1–ETO, and HDAC3 by comparing single and combined knockdown effects on IL8 expression. Depleting RUNX1 alone increased IL8 expression, as expected (Fig. 2*D*, *lane 3*). However, this effect was not further increased by additional depletion of HDAC3 (Fig. 2*D*, *lanes 3* and *7*), indicating that RUNX1 and HDAC3 are both required for optimal repression of IL8 transcription. Furthermore, the stimulatory effects resulting from depleting RUNX1 or HDAC3 required AML1–ETO (Fig. 2*D*, *lanes 2*, *6*, and *8*). This shows that the ability of AML1–ETO to activate IL8 gene transcription was dominantly inhibited by the collaborative functions of RUNX1 and HDAC3, provid-

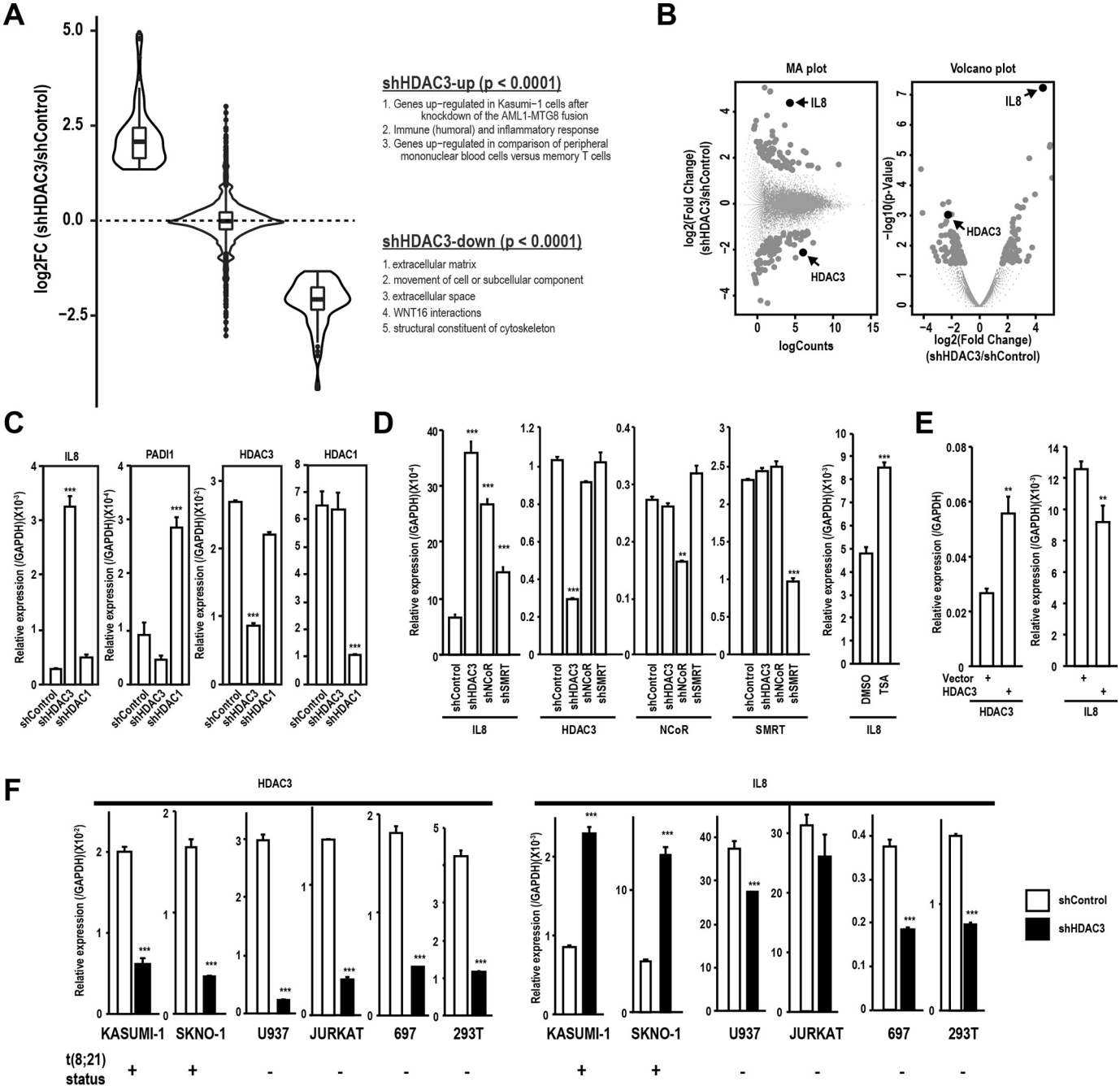

Figure 1. HDAC3 transcriptionally represses the *IL8* gene in t(8;21) AML cells. *A*, fold changes of genes upon depletion of HDAC3 in Kasumi-1 cells, including up-regulation (shHDAC3-up genes), down-regulation (shHDAC3-down genes), and no significant change. The *right panel* shows significantly enriched functions ($p < 0.0001$) for shHDAC3-up and shHDAC3-down genes. *B*, MA and volcano plots of differentially regulated genes, comparing HDAC3-depleted and control Kasumi-1 cells, including IL8 and HDAC3, highlighted here. *C*, RT-qPCR analysis in control (*shControl*), HDAC3 knockdown (*shHDAC3*), and HDAC1 knockdown (*shHDAC1*) Kasumi-1 cells. *D*, RT-qPCR analysis of shControl, shHDAC3, NCoR knockdown (*shNCoR*), and SMRT knockdown (*shSMRT*) Kasumi-1 cells. Also shown are effects of DMSO and TSA treatment on IL8 expression in Kasumi-1 cells, assayed by RT-qPCR. *E*, RT-PCR analysis of Kasumi-1 cells expressing ectopic HDAC3 or an empty vector. *F*, RT-qPCR analyses of HDAC3 and IL8 expression in various t(8;21) and non-t(8;21) cells. **, $p < 0.01$; ***, $p < 0.001$.

ing the first evidence that RUNX1 can also collaborate with HDAC3 to repress AML1–ETO–mediated transcriptional activation. This is analogous to the reported ability of AML1–ETO to collaborate with HDAC3 to repress RUNX1-dependent gene transcription, suggesting that HDAC3 facilitates bidirectional negative interplays between AML1–ETO and RUNX1.

Primary t(8;21) AML samples also show the antagonistic effect between RUNX1–HDAC3 and AML1–ETO

We next examined IL8 levels in 35 cases of t(8;21)-positive primary AML samples (GSE14468). Consistent with a negative role of RUNX1 in regulating IL8 expression in t(8;21) AMLs, a strong negative correlation was observed between RUNX1 expression and IL8 expression ($r = -0.60$, $p = 2.7E-4$, Fig. 3*A*).

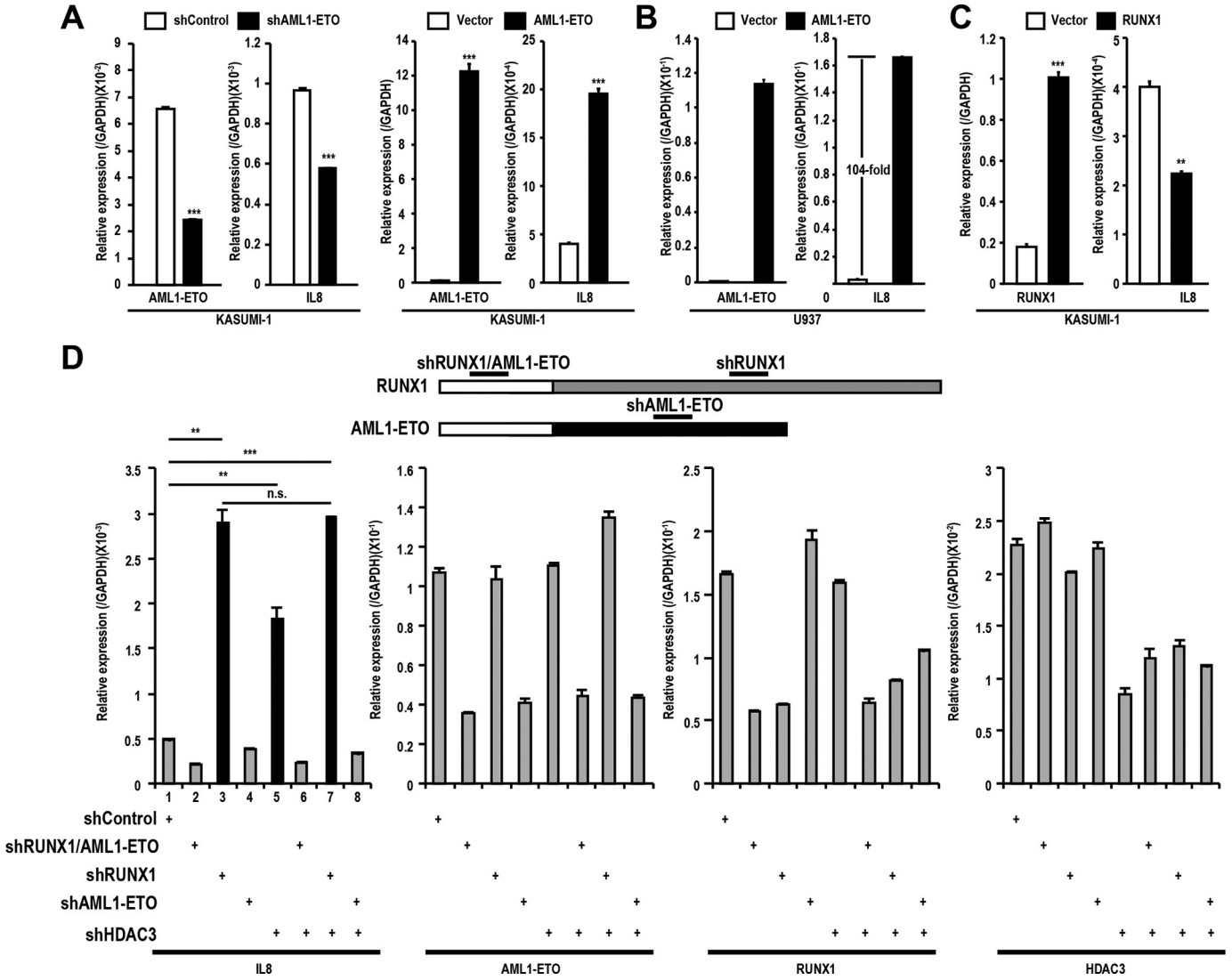

Figure 2. HDAC3 and RUNX1 collaboratively repress AML1–ETO–dependent *IL8* gene transcription. *A*, RT-qPCR analyses of depleting and overexpressing AML1–ETO in Kasumi-1 cells. *B*, RT-qPCR analyses of U937 cells with overexpressed AML1–ETO. *C*, RT-qPCR analyses of Kasumi-1 cells with overexpressed RUNX1. *D*, effects of single and combined knockdown of AML1–ETO, RUNX1, and HDAC3 on the expression of genes indicated at the *bottom* in Kasumi-1 cells. *Top panel*, the location of pan-AML1–ETO/RUNX1 shRNA, RUNX1-specific shRNA, and AML1–ETO–specific shRNA. **, $p < 0.01$; ***, $p < 0.001$; *n.s.*, not significant.

Although HDAC3 only showed a modest negative correlation with IL8 ($r = -0.34$, $p = 0.049$), it enhanced the negative correlation between RUNX1 and IL8, as measured between IL8 expression and the additive expression levels of RUNX1 and HDAC3 ($r = -0.68$, $p = 8.5E{-}6$). In contrast to HDAC3, HDAC1 neither showed a significant correlation with IL8 nor enhanced the correlation between RUNX1 and IL8 (Fig. 3*A*). Contrary to the negative effects seen with RUNX1 and HDAC3, t(8;21) AML samples showed a higher average level of IL8 expression than non-t(8;21) samples (Fig. 3*B*), consistent with the ability of AML1–ETO to activate IL8 gene expression.

To add further confidence to the results, we performed multivariate linear regression, in which we modeled IL8 expression in the t(8;21) samples as a function of RUNX1, AML1–ETO, HDAC3, and HDAC1 expression. The significant negative coefficients of RUNX1 and HDAC3 are consistent with their negative roles in regulating IL8 expression (Fig. 3*C*). As expected, HDAC1 showed a coefficient close to zero, consistent with the lack of its contribution to regulating IL8 expression (Fig. 3*C*). AML1–ETO had a highly positive coefficient (Fig. 3*C*), consistent with its ability to activate IL8 gene expression. Its *p* value, however, did not reach a significant level, which could be caused by other confounding patient-specific variables or the dominant effects of RUNX1 and HDAC3 in regulating IL8.

Consistent with changes in *IL8* mRNA expression, IL8 levels in cell culture media were reduced by depletion of AML1–ETO and increased by depletion of RUNX1 or HDAC3 (Fig. 3*D*). Both HDACs (including HDAC3) and RUNX1 have been reported to promote leukemia progression in t(8;21) AML (28, 29). Given that IL8 is a pro-inflammatory cytokine associated with senescence (30), down-regulation of IL8 may contribute to the leukemia-promoting effects of RUNX1 and HDAC3.

RUNX1 associates with HDAC3/nuclear receptor corepressor complexes

HeLa cells express RUNX1 (31) and have been used to isolate HDAC3 complexes (10). Although our results suggest involve-

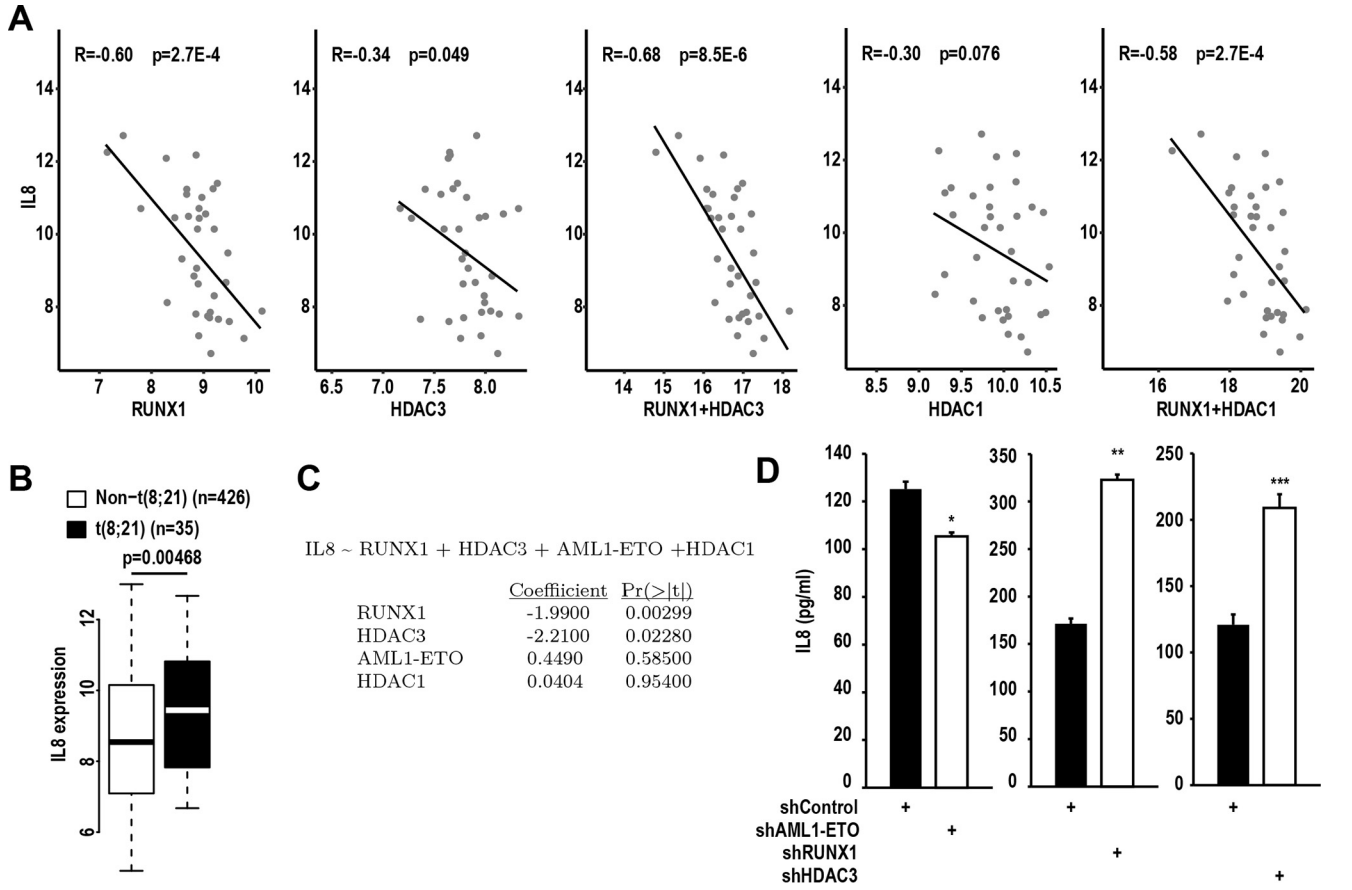

Figure 3. RUNX1–HDAC3 and AML1–ETO opposingly regulate IL8 expression in t(8;21) AML patient samples. *A*, scatterplots showing the correlation of IL8 expression with individual or combined expression of RUNX1, HDAC3, and HDAC1 in the 35 cases of t(8;21) AML samples (GSE14468). *B*, IL8 was expressed at higher levels in t(8;21) than in non-t(8;21) AML samples (GSE14468). *C*, multivariate linear modeling of IL8 expression confirmed the results in *A* and *B*. Linear regression was performed using the lm function in R. *D*, ELISA analyses of IL8 levels in cell culture media of Kasumi-1 cells following knockdown of the indicated genes. *, $p < 0.05$; **, $p < 0.01$; ***, $p < 0.001$.

ment of t(8;21)-specific mechanisms in regulating IL8 expression, this could be due to lack of AML1–ETO–like activators in non-t(8;21) cells. LC-MS/MS and subsequent Western blot analyses showed that RUNX1 (but not p300) was present in the purified HDAC3 complex, which was isolated from stable FLAG–HDAC3– expressing HeLa cells (Fig. 4, *A–C*, and Supporting Information S1 and S2). GST pulldown assays further showed that RUNX1 interacted with HDAC3, whereas the CoR protein SMRT interacted with ETO, as expected (Fig. 4*D*).

Because CoRs are important for the enzymatic activity of HDAC3, we asked whether RUNX1 is capable of associating with CoRs. To this end, we purified FLAG–RUNX1, FLAG–AML1–ETO, and FLAG–AML1–ETO9a complexes from their respective stably expressing HeLa cells. Western blot analysis showed that RUNX1 was associated with HDAC3 complex components, including HDAC3, SMRT, NCoR, TBL1, and GPS2 (Fig. 4*E*), independent of DNA-mediated interactions (Fig. S2). As expected, HDAC3 complex proteins were also present in the AML1–ETO complex but not in the AML1–ETO9a complex, consistent with the lack of NHR4 in AML1–ETO9a (Fig. 4*E*) (32). Significant amounts of the HEB E-protein, which binds to the NHR1/2 regions present in both AML1–ETO and AML1–ETO9a, was detected in AML1–ETO and AML1–ETO9a but not RUNX1 complexes (Fig. 4*E*). Finally, functional HDAC assays showed that the purified RUNX1 complex contained significant histone deacetylase activity (Fig. 4*F*).

To gain further insight into how RUNX1 interacts with HDAC3, we compared the abilities of full-length RUNX1 and its C-terminally truncated derivatives to interact with HDAC3 by coimmunoprecipitation assays. A region between amino acids 269 and 438 containing the activation domain of RUNX1 was required for stable interactions with HDAC3 (Fig. 4*G*). We also examined HDAC3-dependent RUNX1 and SMRT interactions. FLAG-SMRT alone elicited a weak interaction with RUNX1 in transfected HEK293T cells, likely mediated by the endogenous HDAC3, which was also coimmunoprecipitated with FLAG-SMRT (Fig. 4*H*). Further supporting this idea, the interaction between RUNX1 and SMRT was dramatically increased by ectopic expression of HDAC3 (Fig. 4*H*). We also tested the role of GPS2 in mediating SMRT–RUNX1 interactions, given its documented interactions with transcription factors (33). Ectopic GPS2 only modestly increased the interaction between RUNX1 and FLAG-SMRT (Fig. 4*H*). Together, these results suggest that RUNX1 associates with the CoR–HDAC3 complex through the HDAC3 subunit.

Because HDAC3 also associates with AML1–ETO, we next compared the relative binding affinities of HDAC3 for RUNX1 and AML1–ETO by comparative affinity pulldown assays. We first examined these interactions using stable FLAG–HDAC3–

expressing Kasumi-1 cells. FLAG–HDAC3 strongly associated with endogenous SMRT (Fig. 4*I*, *top*), indicating that it behaved as the endogenous protein. An N-terminal RUNX1 antibody was used to simultaneously detect AML1–ETO and RUNX1. Only RUNX1, but not AML1–ETO, was detected in the FLAG–HDAC3 immunoprecipitates. Similar results were observed by examining endogenous interactions in Kasumi-1 cells (Fig. 4*J*). Notably, several putative RUNX1 isoforms were found in the

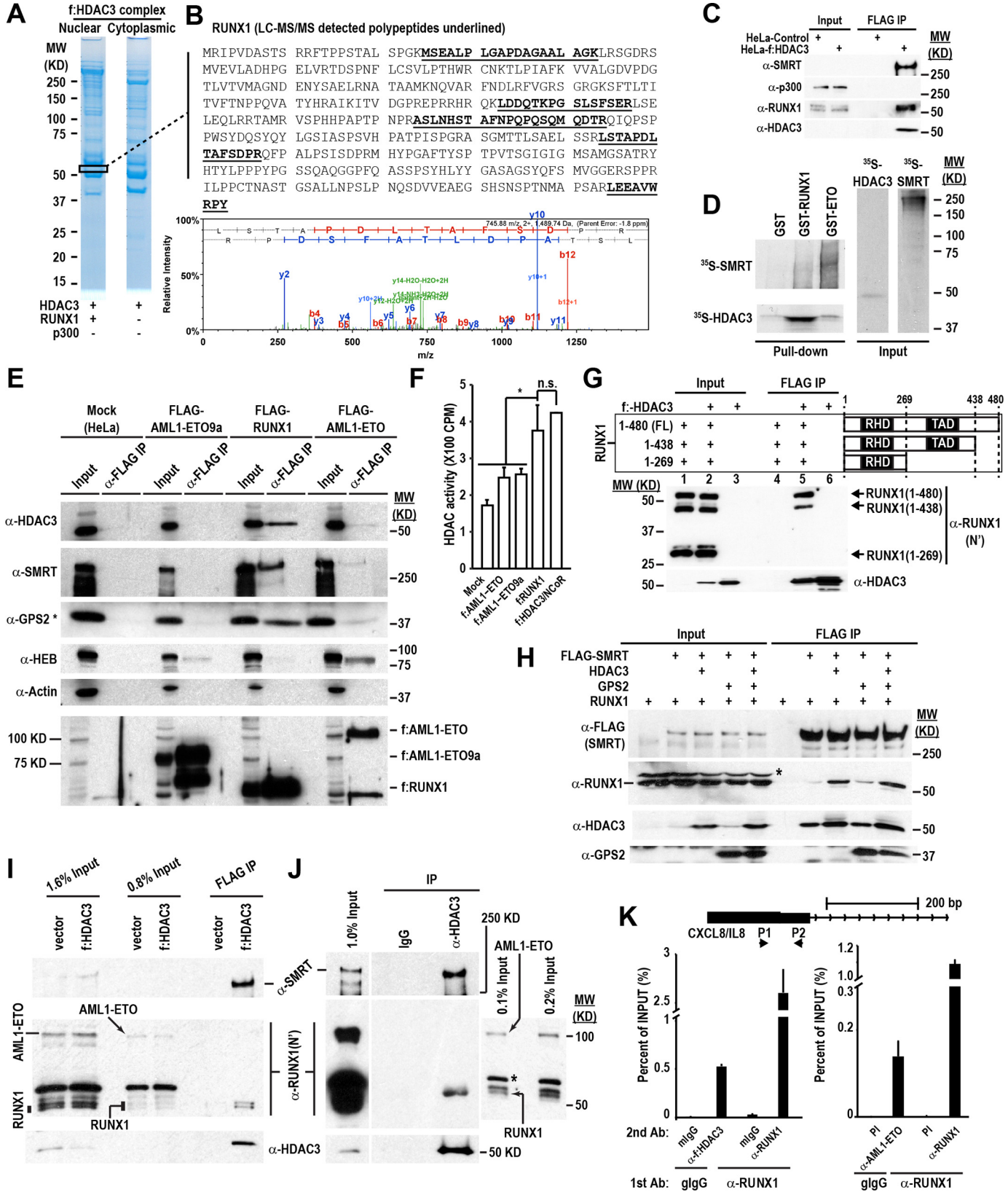

Kasumi-1 cells (Fig. 4, *I* and *J*). Although the nature of these isoforms remains to be further elucidated, those that showed specific interactions with HDAC3 were expressed at levels comparable with that of endogenous AML1–ETO (Fig. 4, *I* and *J*). Together, these results demonstrate that HDAC3 preferentially binds to RUNX1, but not AML1–ETO, in Kasumi-1 t(8;21) AML cells.

We then asked whether RUNX1 and HDAC3 co-occupy the binding sites of target genes by performing re-ChIP assays in FLAG–HDAC3–expressing Kasumi-1 cells. The ChIP-Seq studies described below identified a binding site at the exon 1 region of the IL8 gene (Fig. 6*A* and Fig. S6). Focusing on this site, the re-ChIP assay results confirmed simultaneous binding of RUNX1 and HDAC3 to this IL8 site (Fig. 4*K*, *left*). Similar re-ChIP analyses of AML1–ETO and RUNX1 also documented co-occupancies of RUNX1 and AML1–ETO (Fig. 4*K*, *right*), consistent with the idea that AML1–ETO and RUNX1 can simultaneously bind to AML1–ETO–activated genes.

Paired ChIP-Seq studies reveal genome-wide AML1–ETO–independent chromatin complexes containing RUNX1 and HDAC3

If RUNX1 is capable of independently recruiting HDAC3 to chromatin, then depleting AML1–ETO should not abolish HDAC3 binding at the *IL8* locus. ChIP-Seq studies were performed to test this idea while also generalizing the result to global AML1–ETO target genes. These studies were performed in a paired fashion (*i.e.* in both control and AML1–ETO–depleted Kasumi-1 cells) to systematically compare chromatin occupancies of various transcription factors (AML1–ETO and RUNX1), coregulators (HDAC1, HDAC3, SMRT, p300, and GCN5), RNA polymerase II, and histone marks with and without AML1–ETO. As a validation of the assay, depletion of AML1–ETO almost completely abolished AML1–ETO ChIP-Seq signals (Figs. 5*B* and 6*A* and Figs. S6 and S7). To interrogate changes in chromatin binding with changes in gene expression, we also analyzed a microarray dataset, GSE45743 (34) (Fig. 5*A* and Fig. S3), and obtained a list of high-confidence genes that were antagonistically regulated by AML1–ETO and RUNX1 in Kasumi-1 cells. In the following analysis, we designated these genes as "act" genes, which are activated by AML1–ETO but repressed by RUNX1, and "rep" genes, which are repressed by AML1–ETO but activated by RUNX1. Validating the results of this analysis, IL8 was among the act genes, and RASSF2, which is known to be strongly repressed by AML1–ETO (13), was among the rep genes.

First, ChIP-Seq results at the *IL8* locus confirmed our hypothesis by showing that depletion of AML1–ETO did not abolish HDAC3 binding. In contrast, the binding levels of HDAC3 and SMRT were increased after AML1–ETO depletion (Fig. 6*A* and Fig. S6). Similar effects were observed at the AML1–ETO– binding site of the *RASSF2* gene (Fig. S7). The *IL8* and *RASSF2*-binding sites, however, differed in the changes in RUNX1 binding levels. Although depleting AML1–ETO strongly increased RUNX1 binding at the RASSF2 site (Fig. S7), it only minimally affected RUNX1 binding at the IL8 site (Fig. 6*A* and Fig. S6). These results can be generalized to the total act and rep genes. Although depleting AML1–ETO had a more dramatic effect of increasing the RUNX1, HDAC3, and SMRT binding levels at the rep genes, it showed a lesser effect at the act genes (Fig. 5*B*). Correlation analyses also showed that the changes in binding levels of RUNX1, HDAC3, and SMRT were highly correlated (data not shown). Along with our finding that RUNX1, HDAC3, and SMRT can form a protein complex, these results support the idea that RUNX1 can independently recruit HDAC3 to chromatin, which was also supported by modeling chromatin binding of HDAC3 at act and rep genes using multivariate linear regression (Fig. S4). The differential effects of AML1–ETO depletion on RUNX1 binding levels at rep and act genes are consistent with the proposal (16, 21) that AML1–ETO competes with RUNX1 for DNA binding predominantly at AML1–ETO–repressed (*e.g. RASSF2*) but not AML1–ETO–activated genes (*e.g. IL8*).

Paired ChIP-Seq results also showed that depleting AML1–ETO globally reduced chromatin binding of p300, most evident at act genes (Figs. 5*B* and 6*A* and Figs. S6 and S7), whereas depleting AML1–ETO increased GCN5 binding, most evident at rep genes (Figs. 5*B* and 6*A* and Figs. S6 and S7). These results are consistent with the roles of AML1–ETO in activating transcription by recruiting p300 (6) and in repressing transcription by dismissing GCN5 from E-proteins (12, 13). Further supporting this latter idea, E-proteins were present at the AML1–ETO– binding sites after AML1–ETO depletion (data not shown). The finding that AML1–ETO reduced the occupancy of GCN5 and RUNX1 at rep genes (Fig. 5*B* and Fig. S7) also suggests that the two previously noted mechanisms for AML1–ETO–mediated repression, dismissing RUNX1 from DNA and

Figure 4. RUNX1 physically interacts with the HDAC3–CoR complex and has a higher binding affinity for HDAC3 than that of AML1–ETO in t(8;21) AML cells. *A*, zinc-stained SDS-PAGE gels showing purified FLAG–HDAC3 complexes from nuclear and cytoplasmic fractions of HeLa cells. *Bottom panel*, the presence (+) or absence (−) of HDAC3-, RUNX1-, and p300-derived polypeptides identified by MS/MS. *MW*, molecular weight. *B*, RUNX1 sequence and the location of LC-MS/MS–identified polypeptides (*top panel*) and a representative MS/MS spectrum originated from the RUNX1 polypeptide (*bottom panel*). The list of complete RUNX1-derived peptides and protein assignment can be found in Supporting Information S1 and S2. The assigned protein (runt-related transcription factor 1 isoform AML1b) is an isoform of RUNX1. *C*, Western blot assays of the purified nuclear FLAG–HDAC3 complex. *D*, autoradiography of SDS-PAGE gels showing signals of [^{35}S]SMRT and [^{35}S]HDAC3 after pulldown by immobilized GST, GST-RUNX1, and GST-ETO (*left panel*) and input samples (*right panel*). *E*, Western blot analyses of input and purified FLAG–RUNX1, FLAG–AML1–ETO9a, and FLAG–AML1–ETO complexes from nuclear extracts of engineered HeLa cells. *Asterisk*, α-GPS2 Western blot from a separate gel without an empty lane between different complexes. *IP*, immunoprecipitation. *F*, deacetylase activities of purified complexes in *E*. *HDAC3*–NCoR is a recombinant complex containing HDAC3 and the NCoR deacetylase activation domain (10) that served as the positive control in this assay. *G* and *H*, anti-FLAG immunoprecipitation analyses of HEK293T cells cotransfected with the indicated plasmids. *Asterisk*, nonspecific band. A goat HDAC3 antibody (Santa Cruz Biotechnology, SC-8138) was used to detect FLAG–HDAC3. *I* and *J*, Western blot analyses of anti-FLAG immunoprecipitates of control and FLAG–HDAC3 stably expressing Kasumi-1 cells (*I*) and endogenous HDAC3 immunoprecipitates using a mouse HDAC3 mAb (Millipore Sigma, 05-813) (*J*) from the nuclear extracts of the cells. *Asterisk*, location of a nonspecific band. *Vertical bars* in I and the *bottom arrow* in *J* mark RUNX1 isoforms coimmunoprecipitated with HDAC3. *K*, co-occupancy of RUNX1 with HDAC3 (*left*) and RUNX1 with AML1–ETO (*right*) on a regulatory site of the IL8 gene, assayed by re-ChIP in FLAG–HDAC3 stably expressing Kasumi-1 cells. Goat IgG (*gIgG*), mouse IgG (*mIgG*), and preimmune serum (*PI*) were controls for goat anti-RUNX1, mouse anti-FLAG (FLAG–HDAC3), and anti-AML1–ETO antibodies, respectively. *, $p < 0.05$; *n.s.*, not significant.

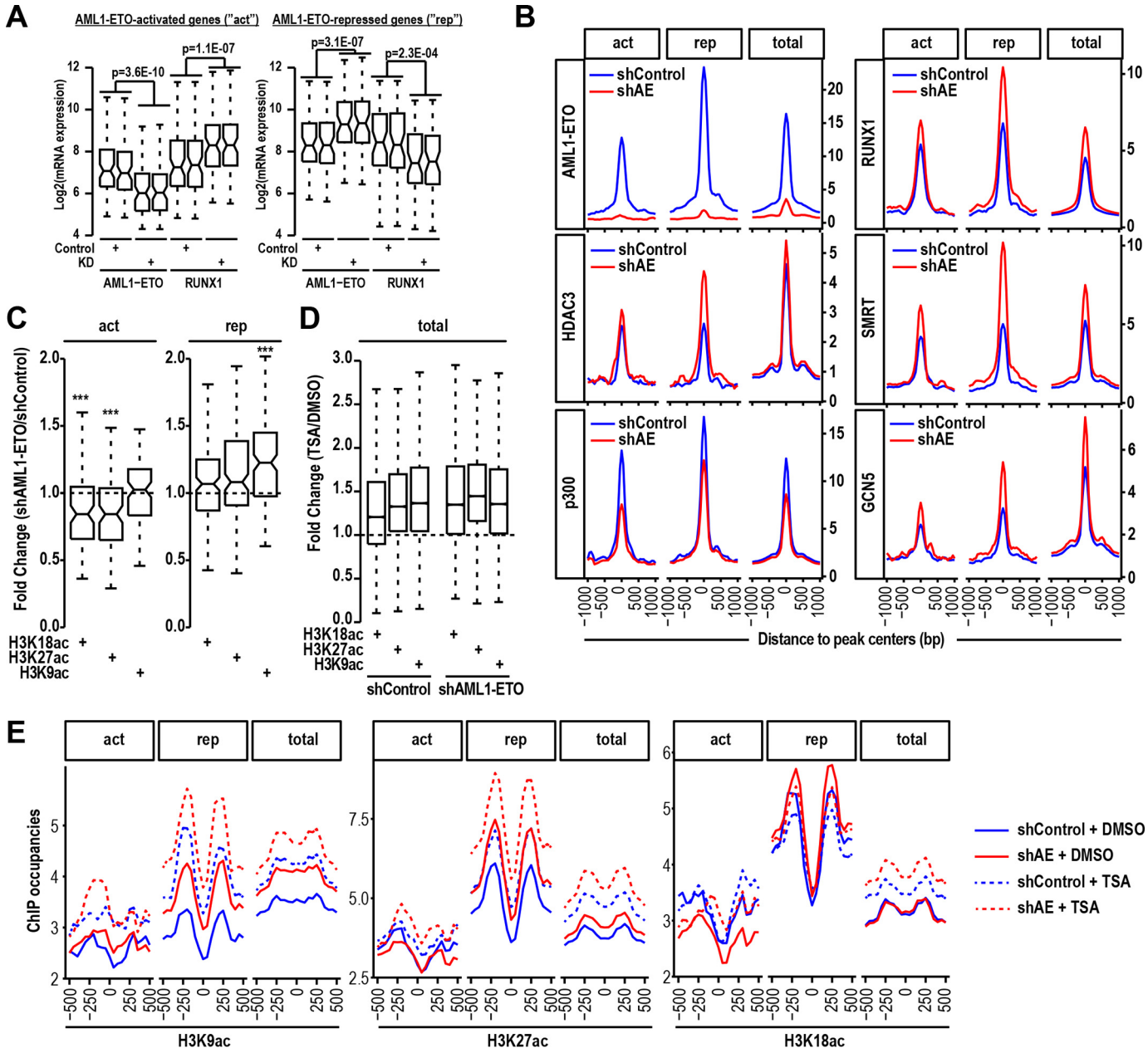

Figure 5. Genome-wide cistrome analyses of paired binding level changes at regulatory sites of genes antagonistically regulated by AML1–ETO and RUNX1 in Kasumi-1 cells. *A*, boxplots of the expression of genes antagonistically regulated by AML1–ETO and RUNX1 in Kasumi-1 cells. The results were analyzed from the GSE45743 dataset. *Control*, control siRNA; *KD*, AML1–ETO– or RUNX1-specific siRNAs. *B*, normalized average binding levels of transcription factors (AML1–ETO (*AE*) and RUNX1), coactivators (p300 and GCN5), and corepressors (HDAC3 and SMRT) at total AML1–ETO binding sites (*total*) and its subset binding sites at act and rep genes in control and AML1–ETO– depleted Kasumi-1 cells. RUNX1 results were analyzed from the public SRP009909 dataset (44). The *X*-axes show distances to peak centers (bp). *C*, fold changes of histone acetylation levels at the binding sites of AML1–ETO at act and rep genes (ratio of shAML1–ETO (*shAE*) *versus* shControl). The data were analyzed from DMSO-treated cells. *p* values were relative to a fold change of 1. *D* and *E*, fold change (*D*) and histogram (*E*) views of histone deacetylation changes under the various treatment conditions, including TSA and AML1–ETO depletion. In *D*, *p* values were relative to a fold change of 1. ***, $p < 0.001$ in *E*, The *X*-axes show distances to peak centers (bp).

dismissing GCN5 from E-proteins, may cooperatively contribute to AML1–ETO–mediated repression.

We also provide evidence that the above-noted changes of chromatin occupancy of transcription factors and coregulators were functionally significant and, in the case of HDACs, were specific for HDAC3, as shown by the expected changes of RNA polymerase II levels at the act and rep genes (Figs. S5–S7 and Fig. 6*A*); the expected changes of histone marks, including p300-dependent acetyl-H3K18/H3K27 and GCN5-dependent acetyl-H3K9 at the act and rep genes, respectively (Fig. 5*C* and Figs. S6 and S7); and the lack of significant binding of HDAC1 at these functional target genes (Figs. S5–S7 and Fig. 6*A*).

Histone deacetylation occurs constitutively in a gene context– and transcriptional state–independent manner

So far, our results suggest that HDAC3, but not HDAC1, is mainly responsible for regulating AML1–ETO target gene transcription in t(8;21) AML cells. This is also supported by our results showing that HDAC3, but not HDAC1, was capable of regulating IL8 in Kasumi-1 cells (Fig. 1*C*). If RUNX1 collabo-

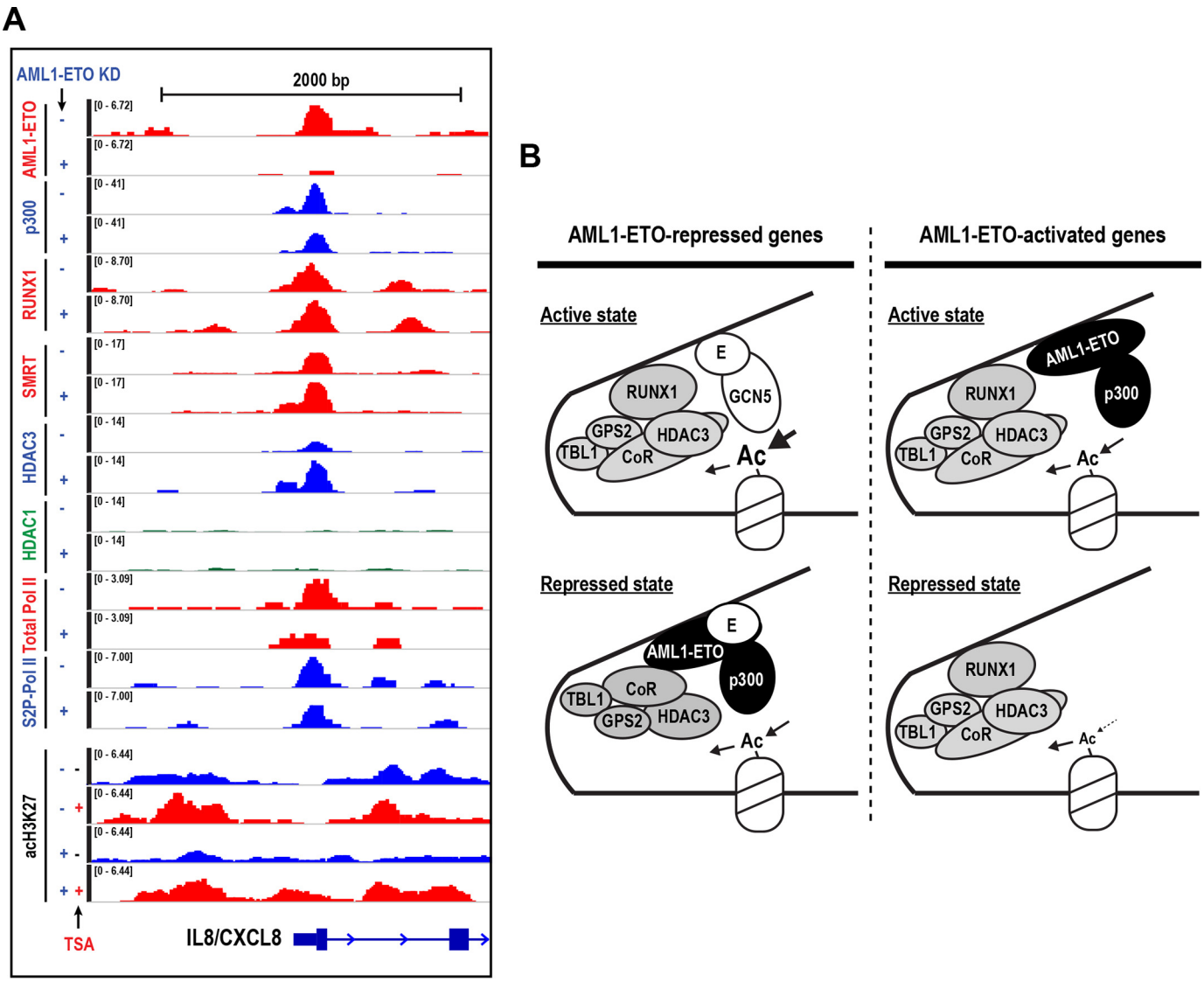

Figure 6. *A*, ChIP-Seq signals of the indicated proteins with and without AML1–ETO depletion and/or TSA treatment at the IL8 gene locus. +, shAML1–ETO or TSA; −, shControl or DMSO. See also Fig. S6. *B*, schematic models based on results obtained in this study. The *left* and *right columns* show AML1–ETO–repressed and AML1–ETO–activated genes, respectively. The *top* and *bottom rows* show compositions of complexes in the active and repressed gene states, respectively. The ChIP-Seq results are consistent with RUNX1–HDAC3–CoR complex formation in three of the transcriptional states, whereas AML1–ETO is responsible for HDAC3–CoR complex recruitment in the repressed state of AML1–ETO–repressed genes. CoR mediates the contact between AML1–ETO and the HDAC3–CoR complex, and HDAC3 plays a role in bridging RUNX1 to the corepressor complex. Our results are consistent with the existence of distinct complex modules at the regulatory loci, including AML1–ETO–p300, E-protein–GCN5, and HDAC3–CoR complexes. The AML1–ETO–p300 module is supported by their reported interaction (6) and the ChIP-Seq results from this study. The competitive binding of AML1–ETO and GCN5 at the rep genes is in line with their competitive interactions with E-proteins, as reported previously (3, 12, 13). Our ChIP-Seq results derived from TSA treatment suggest that histones are constitutively deacetylated at the regulatory sites, likely catalyzed by HDAC3, given its regulated and high-level binding at these sites compared with that of HDAC1. The different levels of steady-state acetyl histones observed at these sites are denoted by the different font sizes of *Ac* (acetyl-lysine), which are likely determined by the balance between HDACs (HDAC3) and histone acetyltransferases (GCN5 or p300). Our results also show that GCN5 plays a dominant role in regulating histone acetylation at the active state of the rep genes, which could result from higher levels of GCN5-mediated histone acetylation (shown here by the *thick arrow*) or, alternatively, reduced levels of histone deacetylation in the presence of GCN5. *E*, E-proteins. The *arrows* next to *Ac* denote deacetylation or acetylation of histones. For simplicity, other factors and cofactors that may also be present at the regulatory sites are not shown, including those catalyzing basal lysine acetylation at the repressed state of the act gene (denoted by a *dashed arrow*).

rates with HDAC3 to repress AML1–ETO– dependent activation of the act genes, then HDAC3 at these loci should be enzymatically active. To test this idea while also exploring the activity of HDAC3 at the various other gene states, we measured the transient changes of histone acetylation after 1-h treatment with Trichostatin A (TSA). We found that TSA treatment globally increased acetyl histone marks (H3K9/H3K18/H3K27) at the AML1–ETO– binding sites, except acetyl-H3K18 at the binding sites of the rep genes (Fig. 5, *D* and *E*, *right panel*), which could possibly be due to a compensatory effect derived from SIRT7 (35), an independent H3K18 deacetylase. These results suggest that histones are constitutively deacetylated across the AML1–ETO cistrome, which may help maintain an appropriate low level of basal transcription while limiting the magnitude of activation. Deacetylation of histones by HDAC3 may be sufficient to control AML1–ETO– dependent p300 functions at the active state (*i.e.* AML1–ETO– bound) of the act genes (Fig. 6*B*, *top right*) and the

repressed state of the rep genes (Fig. 6*B*, *bottom left*). On the other hand, given that both GCN5 and HDAC3/SMRT levels were increased after the rep genes switched from their repressed to the active state upon depletion of AML1–ETO, GCN5 may have a dominant function over that of HDAC3, given the increased steady-state level of acetyl-H3K9 (Fig. 5, *C* and *E*) and the increased transcriptional activity.

Discussion

This study reveals new mechanisms underlying the negative cross-talk between AML1–ETO and RUNX1. These results show, for the first time, that RUNX1 can also collaborate with HDAC3 to negatively regulate the transcription of AML1–ETO–activated genes such as IL8. Combined with the reported role of HDAC3 in facilitating AML1–ETO–mediated repression of RUNX1 target genes, our study reveals that HDAC3 is capable of facilitating bidirectional negative cross-talk between AML1–ETO and RUNX1. Clearly, RUNX1 can also positively regulate AML1–ETO–repressed genes (*i.e.* rep genes), underscoring the importance of studying gene-specific mechanisms in regulating transcription in t(8;21) AML cells.

In contrast to the current model, our study is the first to show that HDAC3 preferentially binds to RUNX1 rather than AML1–ETO in Kasumi-1 t(8;21) AML cells. To our knowledge, this is also the first study to measure endogenous interaction between AML1–ETO and HDAC3 and compare it with that of RUNX1 and HDAC3 using a t(8;21) cell line. Failure to detect an interaction between AML1–ETO and HDAC3 could be related to the stringency of the assay condition, the antibody used, the expression level of the endogenous proteins, or possible competition from RUNX1. We could nevertheless detect the interaction with the CoR–HDAC3 complex using recombinant FLAG–AML1–ETO (Fig. 4*E*). It is possible that binding of AML1–ETO to DNA, especially at rep genes lacking a simultaneously occupied RUNX1, may facilitate stable interactions between AML1–ETO and the CoR–HDAC3 complex.

Although the biological significance of the effect of RUNX1 on AML1–ETO–activated genes remains to be further explored, our finding that, at the molecular level, RUNX1 has the ability to actively repress AML1–ETO– dependent transcription is reminiscent of its dominant effect in antagonizing AML1–ETO's cell arrest activity (34, 36, 37). We thus speculate that, at the biological level, while AML1–ETO inhibition of RUNX1-dependent target gene transcription plays a role in blocking myeloid differentiation, RUNX1 inhibition of AML1–ETO– dependent target gene transcription plays a role in promoting cell survival and growth by allowing RUNX1 to overcome the growth arrest activity of AML1–ETO. It remains to be determined whether the senescence-associated cytokine IL8 is part of these growth-inhibitory pathways.

Competition for DNA binding can explain the AML1–ETO–antagonistic (*i.e.* stimulatory) effect of RUNX1 on expression of AML1–ETO–repressed genes. First, although increased binding of RUNX1 is associated with increased binding of HDAC3 and SMRT, it is also associated with increased binding of GCN5. The net result of these changes is increased histone acetylation. Second, by displacing AML1–ETO from the binding site, a higher stoichiometric ratio of RUNX1 *versus* AML1–ETO should reduce the fraction of rep genes bound to AML1–ETO (Fig. 6*B*, *bottom left*). On the other hand, given that AML1–ETO–activated genes are permissive for co-occupancy by AML1–ETO and RUNX1, competition of DNA binding cannot be used to explain the AML1–ETO–antagonistic (*i.e.* inhibitory) effect of RUNX1 on expression of AML1–ETO–activated genes. In this regard, our finding that RUNX1 uses HDAC3 to repress AML1–ETO–mediated transcriptional activation provides a plausible explanation for how RUNX1 may negatively regulate AML1–ETO–activated genes. These results also support the proposition that, at the act gene loci, RUNX1 functions as a *bona fide* repressor rather than an activator.

Although our results indicate that RUNX1 has a higher binding affinity for HDAC3 than for AML1–ETO, given that RUNX1 is not present in the repressed state of the rep genes, AML1–ETO should be responsible for recruiting HDAC3 to the rep genes under their repressed transcriptional state (Fig. 6*B*, *bottom left*). In addition, the act genes in their active, AML1–ETO– bound state are expected to contain both AML1–ETO and RUNX1 (Fig. 6*B*). Therefore, although AML1–ETO is engaged in association with p300, it may also play a role in stabilizing the overall binding of HDAC3 along with RUNX1 at the AML1–ETO– bound act genes (Fig. 6*B*, *top right*). It is also of note that our histone ChIP-Seq results showed that, unlike the rep genes, depleting AML1–ETO minimally affected the low steady-state levels of the GCN5-specific acetyl-H3K9 mark at the act genes (Fig. 5, *C* and *E*, *left panel*). This suggests that GCN5 does not control the transcription of the act genes, which may allow RUNX1 and HDAC3 to manifest their maximal repressive effects on transcription of the act genes. More studies are needed to further explore these possibilities, including paired ChIP-Seq studies with and without RUNX1 depletion. In this regard, our preliminary result showed that depletion of RUNX1 indeed reduced HDAC3 levels at the IL8 gene binding site (data not shown). It is our belief that a better understanding of the gene-specific mechanisms in assembly and function of the regulatory complexes at both AML1–ETO–repressed and AML1–ETO–activated genes and the molecular bases of the interplays among coactivators and corepressors should greatly advance efforts to decode the language of gene regulation in t(8;21) AML cells and provide new avenues for t(8;21)-specific targeted therapy.

Experimental procedures

Cell culture, shRNA, and plasmids

AML cells were maintained in RPMI 1640 medium with 10% FBS (13). shRNAs (Table S1) were inserted into the pLKO.1 backbone (Sigma). Lentivectors expressing FLAG–AML1–ETO, FLAG–AML–ETO9a, FLAG–RUNX1, and FLAG–HDAC3 have been described or similarly engineered based on coding sequences (12, 17). Plasmids for untagged HDAC3, RUNX1, and RUNX1 mutants were generated by standard molecular cloning technique and verified by Sanger sequencing. Lentiviruses were produced in HEK293T cells (13). FLAG-SMRT was a gift from Dr. Mitchell Lazar.

Gene expression analysis

Quantitative RT-PCR (RT-qPCR) was performed as described previously (13). RNA-Seq was performed at the Genome Technology Access Center Washington University in St. Louis. Differential gene expression analysis of the RNA-Seq dataset and analysis of AML patient samples (GSE14468 (38)) were performed as described previously (12, 39–41).

Protein complex purification and mass spectrometric identification

Protein complexes containing FLAG-tagged HDAC3, AML1–ETO, AML1–ETO9a, and RUNX1 were purified from stably transfected HeLa (S3 clone) cells (10). Following washes, complexes were eluted by FLAG peptide (MilliporeSigma). FLAG-tagged HDAC3 complexes were purified from both nuclear and S100 cytoplasmic fractions and identified following trypsin digestion by LC-MS/MS on an Orbitrap Fusion mass spectrometer (Thermo) as described previously (42). Proteome Discoverer with Sequest (version 2.0.0.802) was used to generate the peak lists and to search the human RefSeq dataset (NCBI; July 6, 2015), which contains 99969 database entries. The search was conducted under 95% or more (peptide) and two or more peptide (protein) threshold levels. The False Discovery Rate (FDR) was controlled at 1.0% (Decoy). Mass tolerance for precursor and fragment ions was 5.0 ppm (monoisotopic) and 0.5 Da (monoisotopic), respectively. Peptides were visualized using the Scaffold 4 software. omplete search parameters can be found in Supporting Information S2.

HDAC assay

^{3}H-labeled *Xenopus* histones prepared via acetylation by recombinant p300 were used for the HDAC assay (3). Released [^{3}H]acetic acid was extracted with ethyl acetate and quantified by liquid scintillation (7).

GST pulldown and coimmunoprecipitation assays

Both assays have been described previously (13).

Measurement of IL8 levels in cell culture media

The RayBiotech Human IL8 ELISA Kit was used to measure IL8 levels in cell culture media after knockdown of HDAC3, RUNX1, and AML1–ETO.

ChIP sequencing (ChIP-Seq) and re-ChIP

ChIP-Seq assays were performed in Kasumi-1 cells transduced with shControl or shAML1–ETO. For histone ChIP-Seq, the cells were additionally treated with DMSO or TSA (100 nM). Peak calling and quantification of ChIP-Seq reads (within a 1-kb region flanking the peak) was performed using HOMER (43). Antibodies for ChIP are shown in Table S1. For re-ChIP, following the first ChIP (13), protein–DNA complexes were dissociated from antibody-immobilized beads by incubation with 50 μl of 10 mM DTT at 37 °C for 30 min, diluted in 350 μl of 1× ChIP buffer, and subjected to a second ChIP.

Statistical analysis

For continuous variables, p values were from Student's t tests unless otherwise noted: *, $p < 0.05$; **, $p < 0.01$; ***, $p < 0.001$; n.s., not significant. p values involving discrete variables, such as gene set enrichment analyses, were from a hypergeometric test.

Author contributions—C. G., J. L., N. S., M. W., B. W., A. D., M. K., and J. Z. data curation; C. G., J. L., N. S., M. W., B. W., A. D., M. K., and J. Z. formal analysis; C. G., J. L., N. S., M. W., B. W., A. D., M. K., and J. Z. validation; C. G., J. L., N. S., M. W., B. W., A. D., M. K., and J. Z. investigation; C. G., J. L., N. S., M. W., B. W., A. D., M. K., and J. Z. methodology; C. G., J. L., N. S., M. W., B. W., A. D., M. K., and J. Z. writing-review and editing; M. K. and J. Z. resources; M. K. and J. Z. software; M. K. and J. Z. funding acquisition; J. Z. conceptualization; J. Z. supervision; J. Z. writing-original draft; J. Z. project administration.

References

1. Miyoshi, H., Kozu, T., Shimizu, K., Enomoto, K., Maseki, N., Kaneko, Y., Kamada, N., and Ohki, M. (1993) The t(8;21) translocation in acute myeloid leukemia results in production of an AML1-MTG8 fusion transcript. *EMBO J.* **12,** 2715–2721 CrossRef Medline
2. Hug, B. A., and Lazar, M. A. (2004) ETO interacting proteins. *Oncogene* **23,** 4270–4274 CrossRef Medline
3. Guo, C., Hu, Q., Yan, C., and Zhang, J. (2009) Multivalent binding of the ETO corepressor to E proteins facilitates dual repression controls targeting chromatin and the basal transcription machinery. *Mol. Cell. Biol.* **29,** 2644–2657 CrossRef Medline
4. Zhang, J., Kalkum, M., Yamamura, S., Chait, B. T., and Roeder, R. G. (2004) E protein silencing by the leukemogenic AML1–ETO fusion protein. *Science* **305,** 1286–1289 CrossRef Medline
5. Sun, X. J., Wang, Z., Wang, L., Jiang, Y., Kost, N., Soong, T. D., Chen, W. Y., Tang, Z., Nakadai, T., Elemento, O., Fischle, W., Melnick, A., Patel, D. J., Nimer, S. D., and Roeder, R. G. (2013) A stable transcription factor complex nucleated by oligomeric AML1–ETO controls leukaemogenesis. *Nature* **500,** 93–97 CrossRef Medline
6. Wang, L., Gural, A., Sun, X. J., Zhao, X., Perna, F., Huang, G., Hatlen, M. A., Vu, L., Liu, F., Xu, H., Asai, T., Xu, H., Deblasio, T., Menendez, S., Voza, F., *et al.* (2011) The leukemogenicity of AML1–ETO is dependent on site-specific lysine acetylation. *Science* **333,** 765–769 CrossRef Medline
7. Gelmetti, V., Zhang, J., Fanelli, M., Minucci, S., Pelicci, P. G., and Lazar, M. A. (1998) Aberrant recruitment of the nuclear receptor corepressor-histone deacetylase complex by the acute myeloid leukemia fusion partner ETO. *Mol. Cell. Biol.* **18,** 7185–7191 CrossRef Medline
8. Lutterbach, B., Westendorf, J. J., Linggi, B., Patten, A., Moniwa, M., Davie, J. R., Huynh, K. D., Bardwell, V. J., Lavinsky, R. M., Rosenfeld, M. G., Glass, C., Seto, E., and Hiebert, S. W. (1998) ETO, a target of t(8;21) in acute leukemia, interacts with the N-CoR and mSin3 corepressors. *Mol. Cell. Biol.* **18,** 7176–7184 CrossRef Medline
9. Wang, J., Hoshino, T., Redner, R. L., Kajigaya, S., and Liu, J. M. (1998) ETO, fusion partner in t(8;21) acute myeloid leukemia, represses transcription by interaction with the human N-CoR/mSin3/HDAC1 complex. *Proc. Natl. Acad. Sci. U.S.A.* **95,** 10860–10865 CrossRef Medline
10. Zhang, J., Kalkum, M., Chait, B. T., and Roeder, R. G. (2002) The N-CoR-HDAC3 nuclear receptor corepressor complex inhibits the JNK pathway through the integral subunit GPS2. *Mol. Cell* **9,** 611–623 CrossRef Medline
11. Guenther, M. G., Barak, O., and Lazar, M. A. (2001) The SMRT and N-CoR corepressors are activating cofactors for histone deacetylase 3. *Mol. Cell. Biol.* **21,** 6091–6101 CrossRef Medline
12. Steinauer, N., Guo, C., Huang, C., Wong, M., Tu, Y., Freter, C. E., and Zhang, J. (2019) Myeloid translocation gene CBFA2T3 directs a relapse gene program and determines patient-specific outcomes in AML. *Blood Adv.* **3,** 1379–1393 CrossRef Medline
13. Gow, C. H., Guo, C., Wang, D., Hu, Q., and Zhang, J. (2014) Differential involvement of E2A-corepressor interactions in distinct leukemogenic pathways. *Nucleic Acids Res.* **42,** 137–152 CrossRef Medline

14. Shia, W. J., Okumura, A. J., Yan, M., Sarkeshik, A., Lo, M. C., Matsuura, S., Komeno, Y., Zhao, X., Nimer, S. D., Yates, J. R., 3rd, and Zhang, D. E. (2012) PRMT1 interacts with AML1–ETO to promote its transcriptional activation and progenitor cell proliferative potential. *Blood* **119,** 4953–4962 CrossRef Medline
15. Chen, M., Zhu, N., Liu, X., Laurent, B., Tang, Z., Eng, R., Shi, Y., Armstrong, S. A., and Roeder, R. G. (2015) JMJD1C is required for the survival of acute myeloid leukemia by functioning as a coactivator for key transcription factors. *Genes Dev.* **29,** 2123–2139 CrossRef Medline
16. Li, Y., Wang, H., Wang, X., Jin, W., Tan, Y., Fang, H., Chen, S., Chen, Z., and Wang, K. (2016) Genome-wide studies identify a novel interplay between AML1 and AML1/ETO in t(8;21) acute myeloid leukemia. *Blood* **127,** 233–242 Medline
17. Meyers, S., Lenny, N., and Hiebert, S. W. (1995) The t(8;21) fusion protein interferes with AML-1B-dependent transcriptional activation. *Mol. Cell. Biol.* **15,** 1974–1982 CrossRef Medline
18. Frank, R., Zhang, J., Uchida, H., Meyers, S., Hiebert, S. W., and Nimer, S. D. (1995) The AML1/ETO fusion protein blocks transactivation of the GM-CSF promoter by AML1B. *Oncogene* **11,** 2667–2674 Medline
19. Westendorf, J. J., Yamamoto, C. M., Lenny, N., Downing, J. R., Selsted, M. E., and Hiebert, S. W. (1998) The t(8;21) fusion product, AML-1-ETO, associates with C/EBP-α, inhibits C/EBP-α-dependent transcription, and blocks granulocytic differentiation. *Mol. Cell. Biol.* **18,** 322–333 CrossRef Medline
20. Ptasinska, A., Assi, S. A., Martinez-Soria, N., Imperato, M. R., Piper, J., Cauchy, P., Pickin, A., James, S. R., Hoogenkamp, M., Williamson, D., Wu, M., Tenen, D. G., Ott, S., Westhead, D. R., Cockerill, P. N., *et al.* (2014) Identification of a dynamic core transcriptional network in t(8;21) AML that regulates differentiation block and self-renewal. *Cell Rep.* **8,** 1974–1988 CrossRef Medline
21. Minucci, S. (2016) DNA binding modes of leukemia oncoproteins. *Blood* **127,** 177–178 CrossRef Medline
22. Guo, H., and Friedman, A. D. (2011) Phosphorylation of RUNX1 by cyclin-dependent kinase reduces direct interaction with HDAC1 and HDAC3. *J. Biol. Chem.* **286,** 208–215 CrossRef Medline
23. Lutterbach, B., Hou, Y., Durst, K. L., and Hiebert, S. W. (1999) The inv(16) encodes an acute myeloid leukemia 1 transcriptional corepressor. *Proc. Natl. Acad. Sci. U.S.A.* **96,** 12822–12827 CrossRef Medline
24. Durst, K. L., Lutterbach, B., Kummalue, T., Friedman, A. D., and Hiebert, S. W. (2003) The inv(16) fusion protein associates with corepressors via a smooth muscle myosin heavy-chain domain. *Mol. Cell. Biol.* **23,** 607–619 CrossRef Medline
25. Chen, X., Barozzi, I., Termanini, A., Prosperini, E., Recchiuti, A., Dalli, J., Mietton, F., Matteoli, G., Hiebert, S., and Natoli, G. (2012) Requirement for the histone deacetylase Hdac3 for the inflammatory gene expression program in macrophages. *Proc. Natl. Acad. Sci. U.S.A.* **109,** E2865–E2874 CrossRef Medline
26. Mullican, S. E., Gaddis, C. A., Alenghat, T., Nair, M. G., Giacomin, P. R., Everett, L. J., Feng, D., Steger, D. J., Schug, J., Artis, D., and Lazar, M. A. (2011) Histone deacetylase 3 is an epigenomic brake in macrophage alternative activation. *Genes Dev.* **25,** 2480–2488 CrossRef Medline
27. Russo, R. C., Garcia, C. C., Teixeira, M. M., and Amaral, F. A. (2014) The CXCL8/IL8 chemokine family and its receptors in inflammatory diseases. *Expert Rev. Clin. Immunol.* **10,** 593–619 CrossRef Medline
28. Sood, R., Kamikubo, Y., and Liu, P. (2017) Role of RUNX1 in hematological malignancies. *Blood* **129,** 2070–2082 CrossRef Medline
29. Gozzini, A., and Santini, V. (2005) Butyrates and decitabine cooperate to induce histone acetylation and granulocytic maturation of t(8;21) acute myeloid leukemia blasts. *Ann. Hematol.* **84,** 54–60 CrossRef Medline
30. Peng, C., Hu, W., Weng, X., Tong, R., Cheng, S., Ding, C., Xiao, H., Lv, Z., Xie, H., Zhou, L., Wu, J., and Zheng, S. (2017) Overexpression of long non-coding RNA PANDA promotes hepatocellular carcinoma by inhibiting senescence associated inflammatory factor IL8. *Sci. Rep.* **7,** 4186 CrossRef Medline
31. Wang, C. Q., Krishnan, V., Tay, L. S., Chin, D. W., Koh, C. P., Chooi, J. Y., Nah, G. S., Du, L., Jacob, B., Yamashita, N., Lai, S. K., Tan, T. Z., Mori, S., Tanuichi, I., Tergaonkar, V., *et al.* (2014) Disruption of Runx1 and Runx3 leads to bone marrow failure and leukemia predisposition due to transcriptional and DNA repair defects. *Cell Rep.* **8,** 767–782 CrossRef Medline
32. Yan, M., Kanbe, E., Peterson, L. F., Boyapati, A., Miao, Y., Wang, Y., Chen, I. M., Chen, Z., Rowley, J. D., Willman, C. L., and Zhang, D. E. (2006) A previously unidentified alternatively spliced isoform of t(8;21) transcript promotes leukemogenesis. *Nat. Med.* **12,** 945–949 CrossRef Medline
33. Wong, M. M., Guo, C., and Zhang, J. (2014) Nuclear receptor corepressor complexes in cancer: mechanism, function and regulation. *Am J. Clin. Exp. Urol.* **2,** 169–187 Medline
34. Ben-Ami, O., Friedman, D., Leshkowitz, D., Goldenberg, D., Orlovsky, K., Pencovich, N., Lotem, J., Tanay, A., and Groner, Y. (2013) Addiction of t(8;21) and inv(16) acute myeloid leukemia to native RUNX1. *Cell Rep.* **4,** 1131–1143 CrossRef Medline
35. Barber, M. F., Michishita-Kioi, E., Xi, Y., Tasselli, L., Kioi, M., Moqtaderi, Z., Tennen, R. I., Paredes, S., Young, N. L., Chen, K., Struhl, K., Garcia, B. A., Gozani, O., Li, W., and Chua, K. F. (2012) SIRT7 links H3K18 deacetylation to maintenance of oncogenic transformation. *Nature* **487,** 114–118 CrossRef Medline
36. Goyama, S., Schibler, J., Cunningham, L., Zhang, Y., Rao, Y., Nishimoto, N., Nakagawa, M., Olsson, A., Wunderlich, M., Link, K. A., Mizukawa, B., Grimes, H. L., Kurokawa, M., Liu, P. P., Huang, G., and Mulloy, J. C. (2013) Transcription factor RUNX1 promotes survival of acute myeloid leukemia cells. *J. Clin. Invest.* **123,** 3876–3888 CrossRef Medline
37. Mandoli, A., Singh, A. A., Prange, K. H. M., Tijchon, E., Oerlemans, M., Dirks, R., Ter Huurne, M., Wierenga, A. T. J., Janssen-Megens, E. M., Berentsen, K., Sharifi, N., Kim, B., Matarese, F., Nguyen, L. N., Hubner, N. C., *et al.* (2016) The hematopoietic transcription factors RUNX1 and ERG prevent AML1–ETO oncogene overexpression and onset of the apoptosis program in t(8;21) AMLs. *Cell Rep.* **17,** 2087–2100 CrossRef Medline
38. Wouters, B. J., Löwenberg, B., Erpelinck-Verschueren, C. A., van Putten, W. L., Valk, P. J., and Delwel, R. (2009) Double CEBPA mutations, but not single CEBPA mutations, define a subgroup of acute myeloid leukemia with a distinctive gene expression profile that is uniquely associated with a favorable outcome. *Blood* **113,** 3088–3091 CrossRef Medline
39. Bray, N. L., Pimentel, H., Melsted, P., and Pachter, L. (2016) Near-optimal probabilistic RNA-seq quantification. *Nat. Biotechnol.* **34,** 525–527 CrossRef Medline
40. Robinson, M. D., McCarthy, D. J., and Smyth, G. K. (2010) edgeR: a Bioconductor package for differential expression analysis of digital gene expression data. *Bioinformatics* **26,** 139–140 CrossRef Medline
41. Haas, B. J., Papanicolaou, A., Yassour, M., Grabherr, M., Blood, P. D., Bowden, J., Couger, M. B., Eccles, D., Li, B., Lieber, M., MacManes, M. D., Ott, M., Orvis, J., Pochet, N., Strozzi, F., *et al.* (2013) *De novo* transcript sequence reconstruction from RNA-seq using the Trinity platform for reference generation and analysis. *Nat. Protoc.* **8,** 1494–1512 CrossRef Medline
42. Chiang, A. J., Malli Mohan, G. B., Singh, N. K., Vaishampayan, P. A., Kalkum, M., and Venkateswaran, K. (2019) Alteration of proteomes in first-generation cultures of *Bacillus pumilus* spores exposed to outer space. *mSystems* **4,** CrossRef Medline
43. Heinz, S., Benner, C., Spann, N., Bertolino, E., Lin, Y. C., Laslo, P., Cheng, J. X., Murre, C., Singh, H., and Glass, C. K. (2010) Simple combinations of lineage-determining transcription factors prime *cis*-regulatory elements required for macrophage and B cell identities. *Mol. Cell* **38,** 576–589 CrossRef Medline
44. Ptasinska, A., Assi, S. A., Mannari, D., James, S. R., Williamson, D., Dunne, J., Hoogenkamp, M., Wu, M., Care, M., McNeill, H., Cauchy, P., Cullen, M., Tooze, R. M., Tenen, D. G., Young, B. D., *et al.* (2012) Depletion of RUNX1/ETO in t(8;21) AML cells leads to genome-wide changes in chromatin structure and transcription factor binding. *Leukemia* **26,** 1829–1841 CrossRef Medline